DEVELOPMENT OF A DYNAMIC MULTIBODY MODEL TO ANALYZE HUMAN LOWER EXTREMITY IMPACT RESPONSE AND INJURY

G.W. Hall [1*], J.R. Crandall [1], W.D. Pilkey [1], J.G. Thunnissen [2]

1) University of Virginia Automobile Safety Laboratory, Charlottesville, VA, USA.
2) TNO Road-Vehicles Research Institute, Delft, The Netherlands.
* Currently at Exponent Failure Analysis Associates, Menlo Park, CA, USA.

ABSTRACT

A dynamic multibody model of the 50th percentile male lower extremity is developed to examine internal loading during plantar impact. The foot and leg, represented by five and seven rigid bodies respectively, are provided with degrees of freedom and stiffness values from cadaveric and volunteer data. Soft tissue structures, including the heel pad, ankle ligaments, and triceps surae muscles are represented with nonlinear viscoelastic elements. Validation involved subjecting the model to two different plantar impact scenarios and comparing the time histories of tibia compression, Achilles tendon tension, and ankle motion with those from the cadaveric test data. Injuries are predicted in the model by comparing force within the model elements with experimentally determined and published failure criteria for the respective structures. This model provides a tool for predicting soft tissue and hard tissue lower extremity injuries associated with a variety of foot and ankle loading environments.

ANKLE INJURIES ARE common (Hurwitz, 1995) and debilitating (Luchter, 1995). These injuries have been studied experimentally, clinically, and statistically to improve our understanding of lower extremity injury mechanisms and patterns. A logical extension of these research efforts is the development of a computational model, where injury and the risk of injury of the lower extremity can be predicted quickly for a variety of loading scenarios.

Modeling efforts to study the human lower extremity have stemmed from two methods, the finite element method (FEM) and the dynamic multibody method. FEM has the advantage of calculating stress distributions within each structure but is severely limited by the current lack of tissue constitutive data. Another challenge with the FEM is creating biofidelic motion at the joints resulting from contact between articular surfaces.

A multibody model simulates the human lower extremity with a linkage of rigid bodies. This modeling method lends itself well to the simulating dynamic events because it directly calculates the parameters that are measured experimentally, such as acceleration, load, displacement, etc. with less computational time relative to FEM models. The development of a multibody model is simpler than developing an FEM model because it is not dependent on the morphology and material properties of the structure being modeled; rather, it only depends on the inertial properties, mechanical structural properties, and connectivity between each rigid body.

Parenteau (1996) used a multibody model to study response of the human lower extremity in an impact environment. In this model, the Hybrid III crash

dummy femur and leg were used with a modified Hybrid III foot and ankle. The contributions of the ankle ligaments and stability afforded by the ankle mortise were lumped into a Cardan stiffness function for the ankle joint. Several ankle ligaments were individually modeled as belt elements with a stiffness function based on quasi-static tension test data. Contributions from the Achilles tendon and triceps surae muscles were not included. The Parenteau model was designed to reproduce the external kinematics of a human leg during quasistatic rotational loading and during axial plantar impact. It was not necessary for the Parenteau model to simulate the internal load-sharing between the tibia, fibula, and triceps surae muscles.

The aim of this research is to create a model that can be used in predicting both external kinematics and hard and soft tissue injury to the human lower extremity resulting from oblique plantar impact. To achieve this goal, it was necessary to include commonly injured structures (ligaments, and malleoli) in the model and provide these structures with a means of assessing injury risk. This approach involved representing smaller segments of the foot and leg than had been studied before, requiring experimental measurement of the dimensions and inertial properties of the smaller rigid bodies, and the mechanical structural properties of the soft tissue structures that affect ankle joint motion. This paper provides an overview of the human lower extremity model design, the sources of its properties, and the validation results.

MODEL DESCRIPTION

This model simulates the right lower extremity of a seated, 50th percentile male occupant during an automobile crash with toepan intrusion. The femur is attached to the inertial frame with a cylindrical joint, and the foot rests on a plane representing the toepan of an automobile. The effect of occupant bracing on the skeleton is simulated by pulling down on the knee. Intrusion is simulated by translating the toepan towards the lower extremity in the $-X$ direction with a prescribed displacement function (Figure 1).

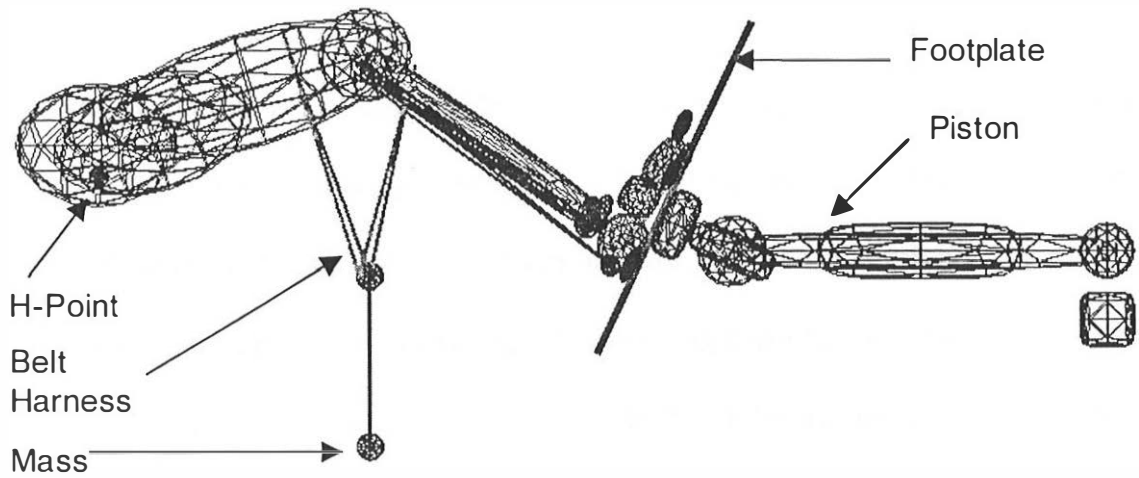

Figure 1 Multibody model environment.

The human lower extremity model has been developed in *MADYMO 5.2* (TNO Road-Vehicles Research Institute, Netherlands) and run on an IBM RS-6000 computer. Integration in the model is performed with the 5th order Runge-Kutta Merson method with variable time step. The average run time is around

100 seconds, but varies with the aggressivity of the impact and the initial orientation of the lower extremity.

Rigid Bodies

The human lower extremity is modeled with eight major segments representing the femur, tibia, fibula, talus, hindfoot, midfoot, tarsals, and toes. Both the fibula and tibia are represented with three rigid bodies each, connected with bracket joints at the mid-diaphysis and distal third (Figure 2). Forces are measured in the model at the bracket joints and used to predict long bone failure during impact based on known fracture force levels. Relative motion between the tibia and fibula is permitted about the X axis of the tibia at the proximal tibia-fibula joint. At the distal ends of the tibia and fibula, contact is defined between the two bones with ellipsoids, and tibiofibular ligament belt elements hold the fibula in place.

The geometry of the leg in the model is that of a 50th percentile male (McConville, 1980). The inertial properties for the tibia, fibula, and muscles of the leg were determined from CT scans by thresholding each slice for the desired tissue (tibia, fibula, muscle) and calculating the mass moment of the tissue about the centroid of the area, assuming constant density. Mass moments of inertia of each of the leg segments were determined by combining the appropriate slices from the CT data. The inertial properties of the soft tissue in the human leg are lumped into the tibia rigid body. The inertial properties and

dimensions of the five foot segments were measured directly from four cadaveric specimens (Table 1).

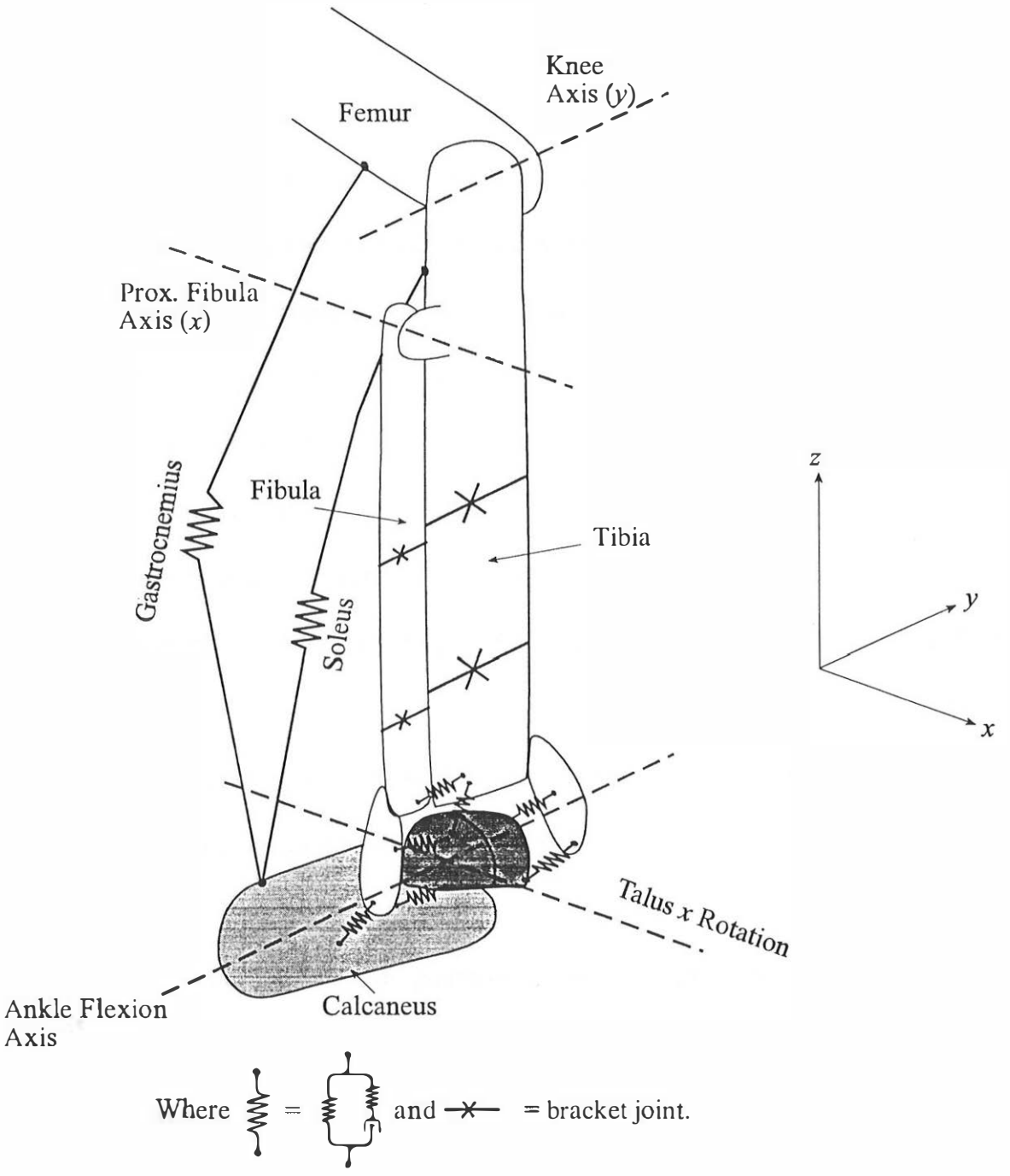

Figure 2 Multibody representation of joints in the multibody leg.

Table 1 Lower extremity model inertial parameters.

	Mass	I_{xx}	I_{yy}	I_{zz}
	(kg)	(kgm^2)	(kgm^2)	(kgm^2)
Tibia upper 1/2	1.856	14.6E-3	14.4E-3	3.10E-3
TIbia middle 1/6	0.714	8.29E-3	8.18E-3	8.07E-4
Tibia lower 1/3	0.315	12.9E-3	12.9E-3	3.78E-4
Fibula upper 1/2	0.077	1.03E-4	1.03E-4	1.15E-6
Fibula middle 1/6	0.057	3.37E-5	3.39E-5	7.42E-7
Fibula lower 1/3	0.020	4.32E-6	4.20E-6	1.75E-7
Talus	0.071	1.11E-5	2.45E-5	2.79E-5
Hindfoot	0.332	2.52E-4	3.61E-4	3.28E-4
Tarsals	0.162	1.78E-4	8.15E-5	1.72E-4
Metatarsals	0.314	3.50E-4	2.35E-4	4.86E-4
Forefoot	0.116	8.69E-5	3.32E-5	10.48E-5

Source: Hall, 1998.

Joints

The knee joint is modeled as a combination revolute and translational joint. The revolute joint is oriented in the *Y* direction of the tibia to approximate the knee flexion axis. The translational joint is oriented along the long axis of the tibia to simulate compliance of the articular surfaces of the knee and the menisci. The orientation and stiffness of the knee and other joints in the model are presented in Table 2.

The ankle (talus to lower tibia) joint is modeled as a universal joint, oriented along the clinical ankle flexion axis (line connecting the distal tips of the medial and lateral malleoli) (Inman, 1976). The first degree of freedom of the universal joint represents dorsiflexion/plantarflexion of the ankle while the second

degree of freedom permits the talus ellipsoid to contact the medial and lateral malleolus ellipsoids. Loading in the fibula results from contact with the talus and tension from the ankle ligaments.

The subtalar joint is modeled as a hinge, oriented 23° about the *Z* axis of the leg, medially from the *X* axis and -42 ± 20.5° about the *Y* axis superior to the *X* axis (Inman, 1976) (Figure 3). The tarsal joint, between the calcaneus and tarsals rigid bodies, is modeled as a ball and socket joint with the same Cardan stiffness functions as used by Parenteau (1996). The tarso-metatarsal joint is oriented along the *Y* axis and assigned an estimated stiffness of 1E+5 Nm/rad, based on expected range of motion. The metatarso-phalangeal (toe) joint is aligned along the ball of the foot (Parham, 1992) and assigned a nonlinear stiffness based on a volunteer study (Hall, 1998).

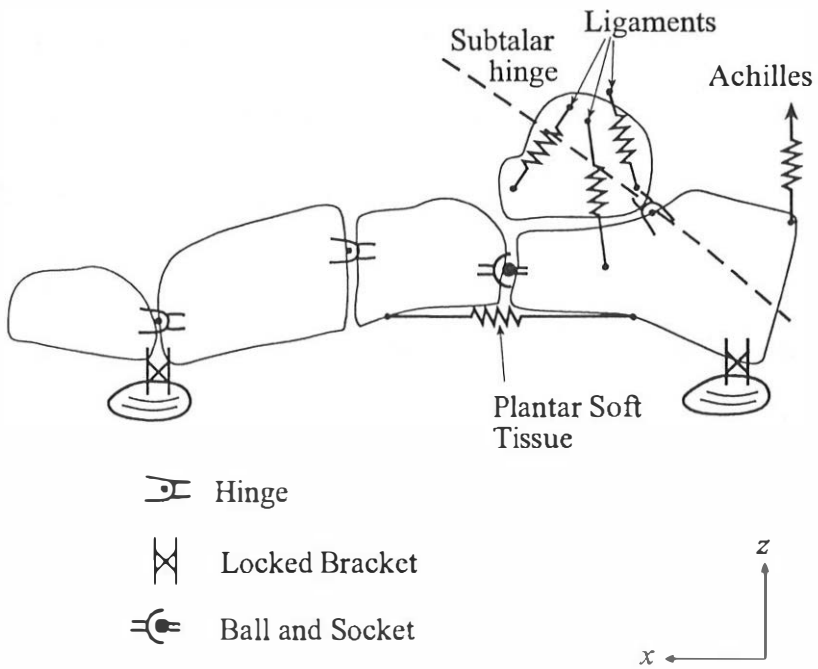

Figure 3 Multibody representation of the joints in the human foot.

Soft Tissues

All soft tissues are modeled with rate sensitive properties based on characterizations performed on 50th percentile male specimens (Hall, 1998). The anterior talofibular, posterior talofibular, calcaneofibular, anterior tibiofibular, posterior tibiofibular, anterior tibiotalar, tibiocalcaneal, and posterior tibiotalar ligaments were characterized individually with quasi-linear viscoelastic (QLV) theory (Fung, 1981) and modeled with a non-linear belt element in parallel with a Maxwell element (Figure 4). The time constant of the Maxwell element represented decay of the ligament in the first 100 milliseconds after a step strain. The non-linear quasi-static stiffness of the ligaments and rate sensitive properties operating on time intervals greater than 100 ms were lumped into the nonlinear belt element because the model is intended for crash studies. The initial slack in each of the ligament belt elements was selected so that each ligament would be tensed to a nominal value (30 N to 50 N) when the ankle and subtalar joints were moved to the limits of the normal range of motion (15° dorsiflexion, 25° plantarflexion, 10° inversion, and 12° eversion). Failure in the ankle ligaments is predicted when the sum of the tension in the ligament belt element and the tension in the ligament Maxwell element exceeds published ligament failure values.

Table 2 Lower extremity model joint orientations and stiffness functions.

	Type	Location/ Orientation	Stiffness
Hip	CYLI	*Y* rotation simulates experimental conditions	Frictionless
Knee	REV	*Y* direction of tibia, rotated 7° from *Y* of femur.	Quasistatic data (TNO-FAT, 1990)
Ankle	UNIV	Midpoint between distal tips of the malleoli, MRI study (Hall, 1998), Orientation from (Inman, 1976)	Quasistatic flexion tests without the Achilles tendon (Schreiber et al., 1995)
Subtalar	REV	Location from dissections (Hall, 1998) Orientation from (Inman ,1976)	Inferred from Kjaersgaard-Anderson et al. (1988)
Midtarsal	BALL	Location from dissections (Hall, 1998) No orientation since BALL	Estimated Cardan stiffness function (Parenteau, 1996)
Tarso-metatarsal	REV	Location from dissections (Hall, 1998) Orientation along *Y* axis	Estimated with 10.0 E+5 Nm/rad based on 10° range of motion
Metatarsal-phalangeal	REV	Line between the 1st and 5th metatarsal-phalangeal joints (Parham et al., 1992)	Nonlinear stiffness from quasistatic volunteer study (Hall, 1998)
Proximal tib-fib	REV	Location from cadaver anthropometry (Hall, 1998) orientation *X* axis	Nonlinear stiffness from quasistatic cadaver study (Hall, 1998)

where: CYLI = cylindrical, REV = revolute, UNIV = universal, and BALL = ball and socket.

The quasi-static, passive stiffness of the gastrocnemius and soleus muscles were determined by pulling the calcaneus away from the femur and tibia, respectively (Hall, 1998). The passive stiffness of these structures is represented in the model with a nonlinear belt element for each muscle. In parallel with the belt element for each muscle is a Maxwell element with a stiffness selected to mimic the Achilles tendon tension measured in cadaveric specimens during plantar impact. Rupture of the Achilles tendon is simulated by

removing the attachment of the Achilles tendon to the calcaneus, based on the resultant force at the Achilles tendon insertion point. Table 3 shows the sources of other soft tissue data.

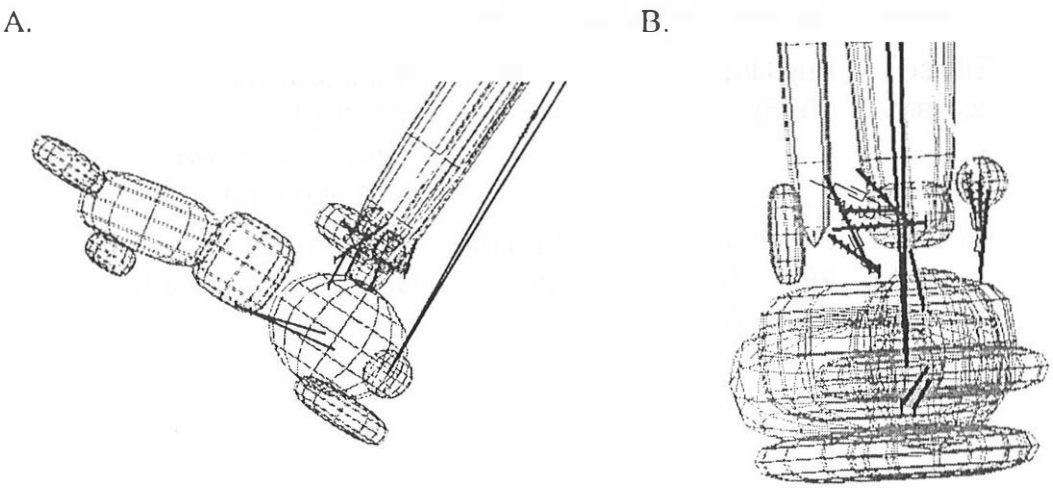

Figure 4 A. Medial-lateral view of foot model. B. Anterior-posterior view of ankle region. Dark lines represent ligaments and muscles.

MODEL ENVIRONMENT

The environment of the current *MADYMO* model was developed to be a flexible platform for examining impact scenarios. The scenarios are queued by selecting an intrusion pulse and the footplate orientation about the *Y* and *X* axes. The model can be run with variable footplate orientations because the leg is not initially in contact with the footplate.

Table 3 Lower extremity model soft tissue properties.

	Type	Location/ Orientation	Characteristics
Ankle ligaments	Belt w/ Maxwell element	Insertions from 50th % male MRI study (Hall, 1998)	Viscoelastic (Hall, 1998)
Gastrocnemius	Belt w/ Maxwell element	Femur insertion 2.0 cm posterior to knee center (Seireg and Arvikar, 1989)	Viscoelastic (Hall, 1998)
Soleus	Belt w/ Maxwell element	Tibia insertion 29 cm proximal to ankle center (Seireg and Arvikar, 1989)	Viscoelastic (Hall, 1998)
Heel pad	Ellipse contact	Fuji film contact data (Hall, 1998)	Nonlinear with respect to compression, one damping value.
Ball pad	Ellipse contact	Fuji film contact data (Hall, 1998) Anthropometry study, (Parham et al.,1992)	Same as heel pad. Contact at 1st and 5th metatarsal

The model begins prior to impact (t = -0.7 seconds) so that the foot can be positioned relative to the footplate. Initially, the lower extremity is suspended with the hip and knee joints locked, and the footplate is pulled in the -*X* direction towards the lower extremity with an acceleration field until the ball and heel of the foot make contact. Contact at the ball of the foot is defined by ellipsoid-plane contact at the first metatarsal head and the fifth metatarsal head. By representing the ball of the foot with two ellipsoids, this configuration permits moments about the *X* axis of the foot to be transmitted into the model. Contact at the heel of the foot is defined by ellipsoid-plane contact between an ellipsoid on the calcaneus, representing the heel fat pad, and the footplate. Compression

failure of the calcaneus is determined by the compressive loads registered between the heel fat pad and the calcaneus. During the pre-impact positioning phase of the model, the hip and knee joints are unlocked after contact between the foot and footplate has been established.

The ankle joint is initially compressed to one half body weight (350 N) to simulate the cadaveric validation test conditions (Hall, 1998). This is accomplished in the model by a belt harness that hangs from the distal femur and proximal tibia with a mass attached. Once the footplate has established contact with the foot, the mass is released, tensioning the belt harness. The mass is locked in place at time equal to -0.01 seconds.

At time zero, the footplate translates with respect to the inertial frame in the $-X$ direction according to a displacement profile from the cadaveric tests. This approach ensures that the foot is impacted the same as in the cadaveric validation experiments. Interaction between the foot and footplate is defined by ellipsoid-plane contact at the heel, 1st metatarsal head, and 5th metatarsal head with a coefficient of friction equal to 0.6.

MODEL VALIDATION AND DISCUSSION

The human lower extremity multibody model was subjected to piston displacement functions from two different experimental scenarios: 1) a low force (3000 N), high onset rate (750 N/ms) test with the ankle initially dorsiflexed 10°; and 2) a high force (6000 N), low onset rate (600 N/ms) test with the ankle

initially plantarflexed 10°. For both loading scenarios, a sample of two cadaveric, male legs were experimentally subjected to plantar impacts. Three primary parameters were used to evaluate the biofidelity of the model: tibia compression, Achilles tendon tension, and ankle dorsiflexion. Figures 5 through 7 compare the response of the model with the cadaveric results for each test condition.

Peak tibia compression is commonly used as a predictor of injury (Mertz, 1993), thus accuracy of the model in predicting this parameter is crucial. The model predicts the peak tibia compression within 9% of the cadaveric mean and the timing of the initial peak within 1.5 milliseconds for both experimental conditions.

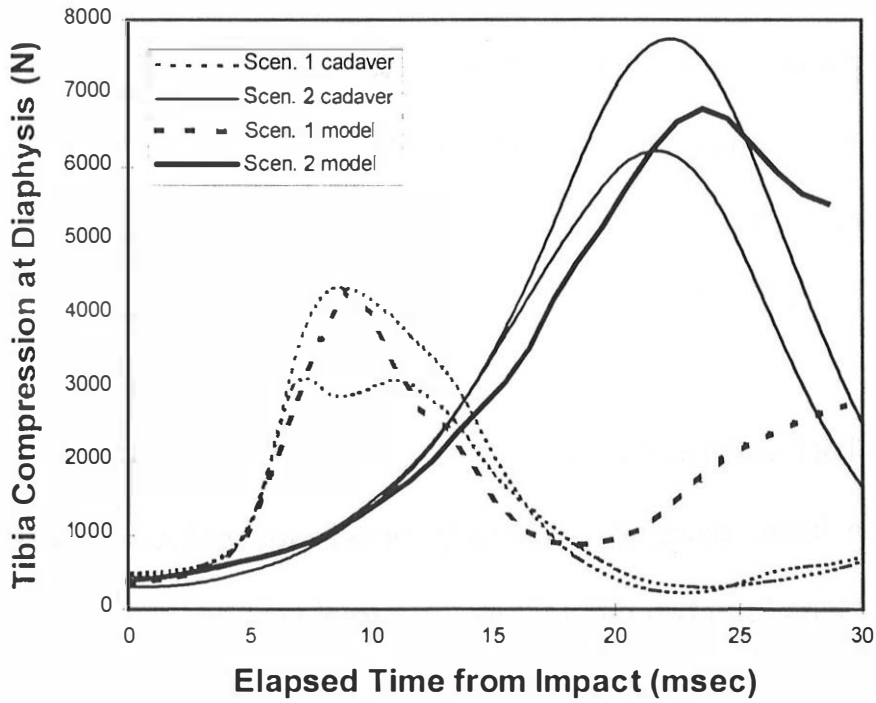

Figure 5 Model prediction of tibia response.

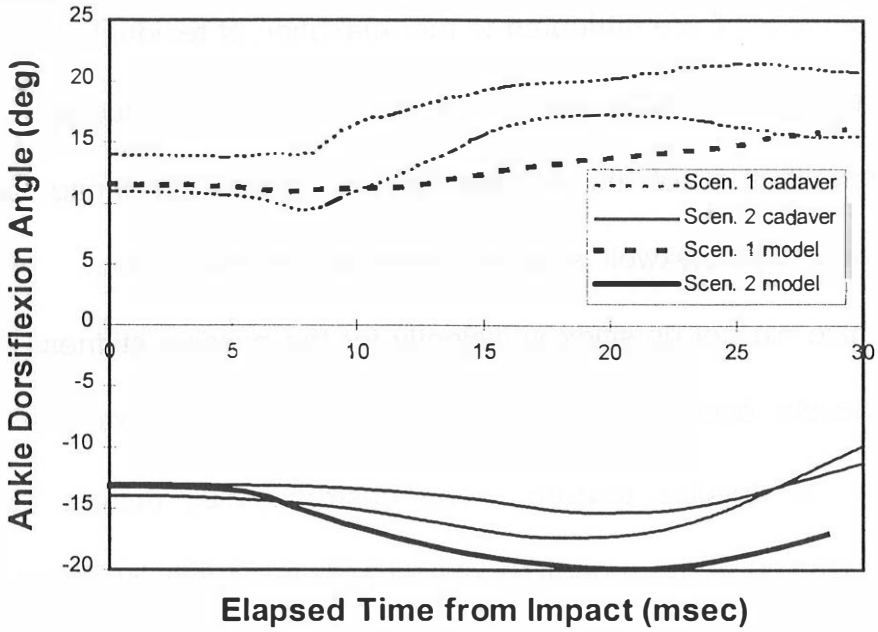

Figure 6 Model prediction of ankle flexion response.

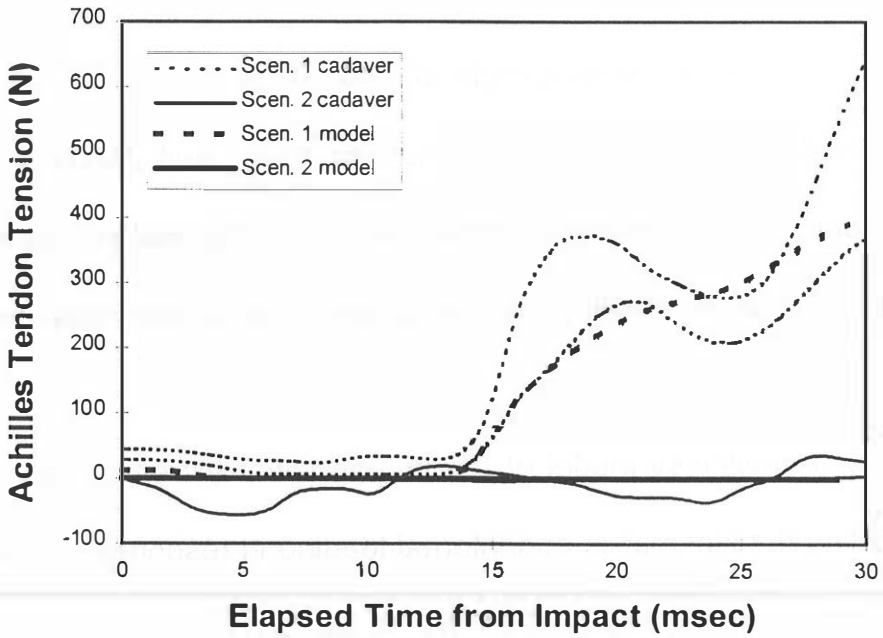

Figure 7 Model prediction of Achilles tendon response.

The model also predicts similar trends to the cadaveric data in ankle motion and Achilles tendon tension. Negative Achilles tension values in the cadaver curves of Figure 7 are attributed to the relaxation of residual stresses in the tendon, unloading the Achilles tension sensor from the reference level. It is interesting to note that all of the Achilles tendon tension for these loading scenarios was from the Maxwell element representing the soleus. In both scenarios, the ankle did not dorsiflex sufficiently for the passive stiffness of the gastrocnemius muscle, occurring at 12° dorsiflexion with a fully extended knee joint (Hall, 1998), to develop tension. The gastrocnemius muscle did not contribute to the loading in the model because the knee is initially flexed, as it would be in an automobile occupant, and intrusion causes the knee to flex further, resulting in a net compression of the passive gastrocnemius, rather than extension.

At the onset of this study, there was concern that the passive Achilles tension during dynamic cadaver testing might affect the tibia compression signal. The model and cadaveric results indicate that for these test conditions on cadaveric specimens, the Achilles tension and tibia peak compression load occur at different times and that the Achilles tension is very small in magnitude when compared to the peak tibia compression.

In summary, a multibody model of the human lower extremity has been created for predicting the kinematics and internal loading in response to oblique plantar impact. The model is capable of predicting fracture in the malleoli, tibia,

fibula, and calcaneus, and rupture of the Achilles tendon and ankle ligaments but awaits accurate, rate-dependent biomechanical data on these parameters. Model prediction of peak tibia compression, ankle motion, and Achilles tension have been validated against experimental cadaveric tests for two impact scenarios. This model will serve in the future to examine new experimental methods and the effects of boundary conditions on leg loading and kinematics.

REFERENCES

Fung, Y. C., Biomechanics: Mechanical Properties of Living Tissues, Springer-Verlag, New York, NY, 1981.

Hall, G. W., "Biomechanical Characterization and Multibody Modeling of the Human Lower Extremity," Ph.D. Thesis, University of Virginia, Charlottesville, VA, 1998.

Hurwitz, S. R., MD., "Clinical Aspects of Foot/Ankle Injuries," Presented at the International Conference on Pelvic and Lower Extremity Injuries (PLEI), Washington, DC, December 5, 1995.

Inman, V., The Joints of the Ankle, Williams and Wilkins Co., Baltimore, 1976.

Luchter, S., "Long Term Consequences of Lower Extremity Injuries," Presented at the International Conference on Pelvic and Lower Extremity Injuries (PLEI), Washington, DC, December 4, 1995.

Kjaersgaard-Anderson, P., Wethelund, J.O., Helmig, P., Soballe, K., "The stabilizing effect of the ligamentous structures in the sinus and canalis tarsi on movements in the hindfoot," *The American Journal of Sports Medicine*, Vol. 16, No. 5, 1988, pp. 512-516.

McConville, J.T., Churchill, T.D., Kaleps, I., Clauser, C.E., Cuzzi, J., Anthropometric Relationship of Body and Body Segment Moment of Inertia. Air Force Aerospace Medical Research Laboratory. Report # AFAMRL-TR-80-119, 1980.

Mertz, H., "Anthropometric Test Devices," Accidental Injury, Biomechanics and Prevention, N. A. Melvin, ed., Springer-Verlag, New York, NY, 1993.

Parenteau, C.S., "Foot-Ankle Joints Responses: Epidemiology, Biomechanics and Mathematical Modeling," Ph.D. Dissertation, Chalmers University of Technology, Goteborg, Sweden, 1996.

Parham, K.R., Gordon, K.C., and Bensel, C.K., "Anthropometry of the Foot and Lower Leg of US Army Soldiers: Fort Jackson, SC – 1985," United States Army Natick Research, Development, and Engineering Center, Natick, MA, September, 1992.

Schreiber, P., Crandall, J. R., Dekel, E., Hall, G. W., Pilkey, W. D., "The Effects of Lower Extremity Boundary Conditions on Ankle Response during Joint Rotation Tests," Proceedings of the 23rd International Workshop on Human Subjects for Biomechanical Research, San Diego, CA, November, 1995.

Seirig A., and Arvikar, R.J., Biomechanical Analysis of the Musculoskeletal Structure for Medicine and Sports, Hemisphere Publishing Corporation, New York, NY, 1989.